33rd Annual International Conference of the IEEE EMBS
Boston, Massachusetts USA, August 30 - September 3, 2011

A Method for Real-Time Cortical Oscillation Detection and Phase-Locked Stimulation

L. Leon Chen, Radhika Madhavan, Benjamin I. Rapoport, and William S. Anderson*

Abstract— **Neural oscillations are important features in a working central nervous system, facilitating efficient communication across large networks of neurons. To better study the role of these oscillations in various cognitive processes, and to be able to build clinical applications around them, accurate and precise estimations of the instantaneous frequency and phase are required. Here, we present methodology based on autoregressive modeling to accomplish this in real time. This allows the targeting of stimulation to a specific phase of a detected oscillation. Using intracranial EEG recorded from two patients performing a Sternberg memory task, we characterize our algorithm's phase-locking performance on physiologic theta oscillations.**

I. Introduction

Neural oscillations are fundamental to the normal functioning of a working central nervous system. There are distinct oscillators in various brain regions that are governed by different physiological mechanisms. For example, prominent oscillations in the theta frequency range can be detected in the hippocampus and entorhinal cortex of rats during locomotion, orienting, conditioning, or while they are performing learning or memory tasks [1], as well as in humans performing various memory and spatial navigation tasks [2], [3]. Because of the role of hippocampal theta oscillations in modulating long-term potentiation (LTP), they are thought to be an important component of memory encoding [4].

The phase of these neural oscillations can possibly be used to store and carry information [5], [6], as well as to modulate physiological activity such as LTP. For example, stimulation applied to the perforant pathway at the peak of hippocampal theta rhythms induced LTP while stimulation applied at the trough induced long-term depression [7]. Theta also serves to temporally organize the firing activity of single neurons involved in memory encoding [8], [9], such that the degree to which single spikes are phase-locked to the theta-frequency field oscillations is predictive of how well the corresponding memory item is transferred to long-term memory [3]. Such temporal patterns of neural activity are potentially important considerations in the design of future neural interface systems. For example, it is plausible that electrical stimulation phase-locked to theta oscillations could either disrupt or augment memory encoding, leading to potentially useful clinical applications.

L. L. Chen, R. Madhavan, and W. S. Anderson* are with the Department of Neurosurgery, Brigham and Women's Hospital, Harvard Medical School, Boston, MA 02115 USA *email: wanderso68@gmail.com

B. I. Rapoport is with the Department of Electrical Engineering and Computer Science, Massachusetts Institute of Technology, Cambridge, MA 02139 USA

Here, we present methods to accurately estimate the instantaneous frequency and phase of an intracranial EEG oscillation signal in real time. At the core of our methodology is an autoregressive model of the EEG signal, which we use to both optimize the bandwidth of the narrow-band signal using estimations of the power spectral density, as well as to perform time-series forward-predictions. These two steps in conjunction allows us to make precise and accurate estimates of the instantaneous frequency and phase of an oscillation, which we then use to target output stimulation pulses to a specific phase of the oscillation.

II. Methods

A. Algorithm Overview

The ultimate goal of our algorithm is to be able to calculate the instantaneous frequency and phase of a neurophysiological signal at a specific point in time with the necessary accuracy and precision to be able to deliver phase-locked stimulation pulses in real time. The algorithm is comprised of several sequential steps depicted in Fig. 1.

B. Autoregressive Model

Autoregressive (AR) modeling provides a robust method of estimating the power spectrum for short (1–2 s) EEG segments, and is less susceptible to spurious results [10]. One issue that is of critical importance in the successful application of AR modeling is the selection of the model order [10], [11]. Because the estimated optimal order varies by the criterion, the sampling rate, and the characteristics of the input data, order selection ultimately depends upon the resulting performance of the system. Thus, it is empirically determined.

C. Frequency Band Optimization

The estimated AR spectrum of a data sequence is a continuous function of frequency and can be evaluated at any given frequency, which is why AR spectral estimation is great at discriminating narrow-band peaks, such as those produced by brain oscillations. Here, the AR model order becomes important in that a low model order will give an overly smoothed spectrum while an overly high order will result in spurious peaks.

To isolate a particular brain oscillation and accurately determine its instantaneous phase, we must perform band-pass filtering around its central frequency. Instantaneous phase only becomes accurate and meaningful if the filter bandwidth is sufficiently narrow [12]. Using predetermined cutoff frequencies may lead to either an insufficiently narrow

978-1-4244-4122-8/11/$26.00 ©2011 IEEE

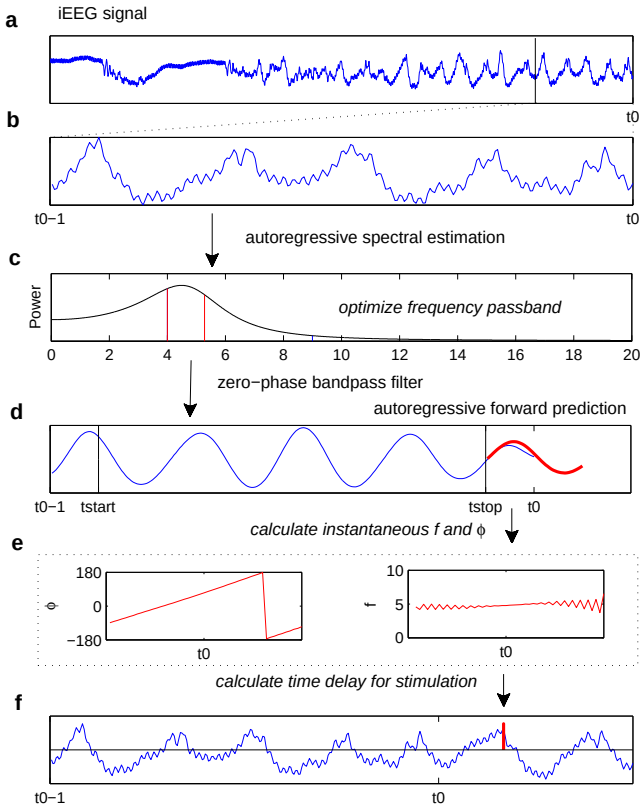

Fig. 1: Overview of algorithm. (a) Raw iEEG signal, where t_0 represents the current time in a real-time acquisition process. (b) Analyze the last 1-second segment of iEEG signal. (c) Use autoregressive spectral estimation to calculate the power spectral density in the 1-second segment. The frequency band optimization procedure is carried out. (d) The 1-second segment is bandpass filtered in both the forward and backward directions, based on the optimized passband. (e) Using the bandpass-filtered signal from t_{start} to t_{stop}, time-series forward predictions (shown in red) are made using the autoregressive model. (f) The instantaneous phase and frequency of this forward-predicted segment are calculated. (g) Using the instantaneous phase and frequency of the forward-predicted segment at t_0, a time delay from t_0 is calculated. Output stimulation is triggered after this time delay (shown in red). Overlaid is the raw iEEG signal from (b) plus some additional time.

band, where noise and extraneous signals will interfere with the brain oscillation signal, or an overly narrow band, in which frequency components of the brain oscillation are lost due to crossing over the range of the passband. Therefore, we developed an adaptive method that optimizes the cutoff frequencies using the AR power spectrum estimate, where the power contained in the optimized band does not fall below a specified threshold level. First, for the raw EEG signal, we calculate the total power contained in a particular frequency band of interest:

$$P(f_L, f_H) = \int_{f_L}^{f_H} S_{\text{AR}}(f)\, df. \tag{1}$$

We then iteratively increase f_L or decrease f_H by a specified step-size δ_f until

$$P(\hat{f}_L, \hat{f}_H) \leq \lambda P(f_L, f_H), \tag{2}$$

where $\hat{f}_L$ and $\hat{f}_H$ are the optimized passband cutoff frequencies, and λ is a fractional multiplier. For every iteration:

$$(\hat{f}_L, \hat{f}_H) = \begin{cases} (f_L + \delta_f, f_H) & \text{if } S_{\text{AR}}(f_L) < S_{\text{AR}}(f_H) \\ (f_L, f_H - \delta_f) & \text{if } S_{\text{AR}}(f_L) \geq S_{\text{AR}}(f_H) \end{cases}. \tag{3}$$

The selection of a value for λ defines the tradeoff between an insufficiently narrow band (λ close to 1) and an overly narrow band (λ close to 0). Here, we set λ to be greater than 0.5, with the justification that we are ensuring the majority of the power contained within the frequency band of interest is contained within the bounds of $\hat{f}_L$ and $\hat{f}_H$. It is important to note that the optimal value of λ may be context-dependent. We are using the assumption that for a particular brain oscillation, there is a certain characteristic frequency, and some amount of variance about that central frequency, rather than the assumption that the oscillation is comprised of many component frequencies. Using this relative measure λ, we are able to ensure that the filter passband is locally optimized within each time segment. A bandpass filter with cutoff bands $\hat{f}_L$ and $\hat{f}_H$ is then applied to the original EEG segment. To prevent phase distortion, we use a zero-phase digital filter that processes input signals in both the forward and reverse directions.

D. Time-Series Forward Prediction

Once we have filtered a signal through the optimized bandpass filter, we can calculate the instantaneous frequency and phase. However, when operating in real time, the relevant $f(t)$ and $\phi(t)$ are its values at the current time, which we will define as t_0. Using a zero-phase filter, distortions will occur near t_0 as only the signal in the reverse direction is available. To make more accurate estimates of $f(t_0)$ and $\phi(t_0)$, we make use of an autoregressive model. For a given EEG segment, we use the bandpass filtered signal from $X_{t_{start}}$ to $X_{t_{stop}}$ to predict a signal of length $2(t_0 - t_{stop})$ from t_{stop} (see Fig. 1). Therefore, the midpoint of this predicted signal corresponds to t_0. We predict a signal of length $2(t_0 - t_{stop})$ to ensure a smooth and continuous instantaneous phase function at t_0, so that the calculation of the instantaneous frequency and phase at t_0 will not be affected by the edge effects of the Hilbert transform. The Hilbert transform will be used to calculate the instantaneous phase and frequency (see section 2E). An example of its edge effect can be seen in the ripples in Fig. 1e.

E. Instantaneous Phase and Frequency

The instantaneous phase is calculated from the complex analytic signal, a combination of the original data and

its Hilbert transform. The instantaneous frequency is then calculated using the derivative of the instantaneous phase.

In our algorithm, the two steps that are based on autoregressive modeling, frequency band optimization and time-series forward prediction, are strategies to attempt to maximize the accuracy of instantaneous phase and frequency estimations.

F. Implementation

Our algorithm was implemented in MATLAB 7.11 (MathWorks, Natick, MA).

The maximum signal segment analysis rate (which translates to the maximum stimulation rate) for the determination of stimulation timing should be greater than the frequency of the oscillation of interest. However, if this frequency is set too high, then spurious outputs will be generated. For theta oscillations, we have set this frequency to be 10 Hz, corresponding to a time window shift every 100 ms. For every period of this analysis cycle, $f(t_0)$ and $\phi(t_0)$ are calculated, and the time delay until the output stimulation is delivered is calculated by the following formula:

$$t_{\text{delay}} = \frac{1}{f(t_0)} \frac{(\varphi - \phi(t_0) + 2\pi) \bmod 2\pi}{2\pi}, \qquad (4)$$

where φ is the desired phase of the output stimulation ($\varphi = 0$ corresponds to the waveform peak, while $\varphi = \pi$ corresponds to the trough). Note that 2π is added as the output of ϕ lies in the interval $(-\pi, \pi]$.

G. Patients and Data

We assessed phase-locking accuracy on physiologic theta oscillations from two epilepsy patients performing a memory task (a version of the Sternberg task adapted from [13], with four list items and a probe item), who had been surgically implanted with subdural electrodes. Informed consent was obtained from the subjects prior to the surgical implantation. Subject 1 had electrodes covering the frontal, parietal and subtemporal areas (73 channels). Subject 2 had electrodes covering the middle, inferior and subtemporal regions (38 channels). We obtained 40 trials from subject 1 and 11 trials from subject 2. Both the correct and incorrect trials were pooled for this analysis. Intracranial (iEEG) signals were recorded from grids and strips electrode arrays.

We optimized the algorithm parameters on the first trial for subject 1 with the single electrode with the largest average theta power. We then used these parameters to perform simulation runs on all electrode channels in subject 1 for all subsequent trials (trials 2–40). Phase-locking performance was assessed at each electrode channel (1–73) collectively over trials 2–40. These same parameters were then tested on subject 2 at each electrode channel (1–38) and assessed collectively over all trials (1–11).

H. Assessment of Phase-Locking Performance

We are interested in two measures of phase-locking accuracy. The first is the difference between the mean stimulation phase $\bar{\phi}$ and the desired phase φ. The second is the variance of stimulation phases. Because not every channel may provide a suitable input signal, we looked at phase-locking performance in the context of the electrode channel's theta power level and theta temporal coherence. The temporal coherence τ_c is calculated by determining the length of time it takes for the amplitude of the autocorrelation function of the theta-bandpassed signal to decrease to half the maximal value at $t = 0$. As an example, for a 1-second truncated sine wave segment, $\tau_c = 0.5$ seconds. We placed electrode channels into four bins: high theta power/high theta coherence, high theta power/low theta coherence, low theta power/high theta coherence, and low theta power/low theta coherence. Electrode channels that did not produce stimulation output were discarded. High theta power was defined as being greater than the median theta power across all remaining electrodes, whereas high theta coherence was defined as being greater than the midpoint of the range of τ_c values. The theta power for each electrode was averaged over trials 2–40 for subject 1 and trials 1–11 for subject 2.

I. Optimizing Parameters Using a Genetic Algorithm

There are multiple parameters in our algorithm that require selection and optimization. Because these variables interact in non-obvious ways, depending on, most of all, the characteristics of the input data, we sought to optimize these parameters simultaneously using a genetic algorithm. The five parameters to be optimized include the AR order p, λ for frequency band optimization, the bandpass filter order and type, and the length $t_0 - t_{stop}$ for time-series forward prediction. Fitness was measured by phase-locking accuracy and precision, as well as a low AR model order.

III. Results

A. Sternberg Task

For subject 1, in the first trial, electrode 45 had the largest average theta power (2300 μV^2), and thus the algorithm parameters were optimized on this data. The resulting optimized parameters are: AR order 22, $\lambda = 0.79$, 2nd order Chebyshev filter, and $t_0 - t_{stop} = 0.05$. Results of simulation runs on trials 2–40 are shown in Fig. 2a. Not all electrode channels had equal phase-locking performance. Channels with both high theta power and high theta temporal coherence resulted in the best performance. The median theta power averaged across trials 2–40 was 570 μV^2, and the theta temporal coherence τ_c averaged across trials 2–40 ranged from 0.0812 to 0.1308 seconds.

The same parameters from subject 1 were tested on subject 2. Out of 38 electrodes, 26 generated output stimulation, and for these electrodes, the median theta power averaged across trials 1–11 was 1500 μV^2 and the theta coherence averaged across trials 1–11 ranged from 0.0690 to 0.1087 seconds. Results are shown in Fig. 2b. Here, electrode channels with both high theta power and high theta temporal coherence resulted in the best performance. Furthermore, it appears that high theta temporal coherence is more important than high theta power.

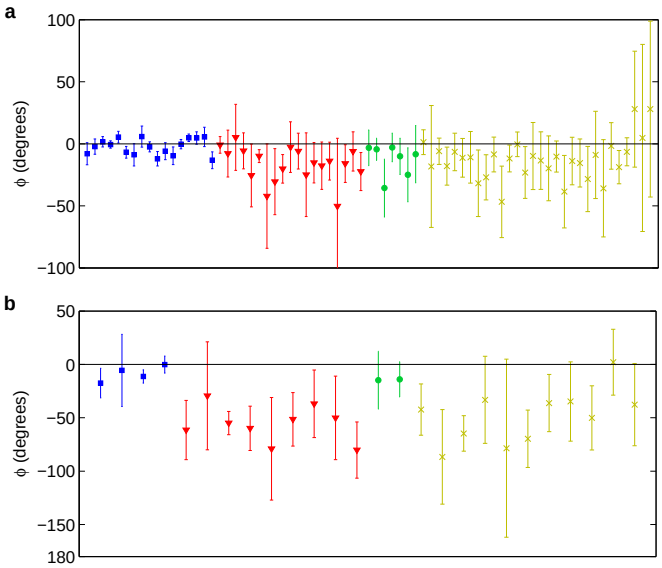

Fig. 2: Phase-locking performance on signals recorded during the Sternberg task ($\bar{\phi}$, error bars represent the 95% confidence interval for $\bar{\phi}$). Electrodes are sorted by high theta power/high theta coherence (blue squares), high theta power/low theta coherence (red triangles), low theta power/high theta coherence (green circles), and low theta power/low theta coherence (yellow crosses). (a) For subject 1, signals from 73 out of 73 electrodes generated output stimulation cumulatively over 39 trials (2–40). (b) For subject 2, signals from 26 out of 38 electrodes generated output stimulation cumulatively over 11 trials (1-11).

These results show that while both high theta power and high theta temporal coherence are important in determining performance, high theta temporal coherence is the more important factor. For example, while channel 18 in subject 2 exhibited very large theta power (5740 μV^2), it exhibited relatively low theta temporal coherence (0.0806 seconds), and thus performed very poorly. On the other hand, channel 20 exhibited lower theta power (1508 μV^2), but had higher theta temporal coherence (0.1087 seconds), which explains its better performance.

IV. Discussion

We have presented here a system for brain oscillation detection and phase-locked stimulation. Though we have tested our system only on theta oscillations, this system can conceivably be used to also study oscillations in other frequency bands. Autoregressive modeling provides an excellent method to estimate the instantaneous frequency and phase, from which we can accurately deliver phase-locked stimulation in real time.

Optimal selection of the AR model order and other algorithm parameters are important considerations. Because these parameters interact with each other and the input data, we used a genetic algorithm method to optimize these parameters simultaneously. This optimization procedure requires intensive computational resources, and thus cannot be done in real time. It must be manually performed on a separate experimental trial (or set of trials) before the algorithm can be deployed. Here, in subject 1 performing the Sternberg task, we performed this optimization on the first trial and used the parameters derived from this optimization on subsequent trials. In subject 2, we used the parameters that were optimized on subject 1. In reality, it may be more appropriate to optimize the parameters on a patient-by-patient basis, as there will be subtle differences in the physiology between patients, such as in the dominant theta frequencies, timing, and spatial characteristics. For example, hippocampi will differ between patients, especially in the presence of underlying pathology such as mesial temporal sclerosis. In addition, our system may further be improved upon in the future by adopting an online adaptive strategy in selecting algorithm parameters, rather than performing an offline optimization procedure prior to online operation.

References

[1] J. O'Keefe and M. L. Recce, "Phase relationship between hippocampal place units and the EEG theta rhythm," *Hippocampus*, vol. 3, no. 3, pp. 317–330, 1993.

[2] M. J. Kahana, "The cognitive correlates of human brain oscillations," *J. Neurosci.*, vol. 26, no. 6, pp. 1669–1672, 2006.

[3] U. Rutishauser, I. B. Ross, A. N. Mamelak, and E. M. Schuman, "Human memory strength is predicted by theta-frequency phase-locking of single neurons," *Nature*, vol. 464, no. 7290, pp. 903–907, 2010.

[4] H. McCartney, A. D. Johnson, Z. M. Weil, and B. Givens, "Theta reset produces optimal conditions for long-term potentiation," *Hippocampus*, vol. 14, no. 6, pp. 684–687, 2004.

[5] K. D. Harris, J. Csicsvari, H. Hirase, G. Dragoi, and G. Buzsaki, "Organization of cell assemblies in the hippocampus," *Nature*, vol. 424, no. 6948, pp. 552–556, 2003.

[6] G. Buzsaki and A. Draguhn, "Neuronal oscillations in cortical networks," *Science*, vol. 304, no. 5679, pp. 1926–1929, 2004.

[7] J. M. Hyman, B. P. Wyble, V. Goyal, C. A. Rossi, and M. E. Hasselmo, "Stimulation in hippocampal region CA1 in behaving rats yields long-term potentiation when delivered to the peak of theta and long-term depression when delivered to the trough," *J. Neurosci.*, vol. 23, no. 37, pp. 11 725–11 731, 2003.

[8] H. Lee, G. V. Simpson, N. K. Logothetis, and G. Rainer, "Phase locking of single neuron activity to theta oscillations during working memory in monkey extrastriate visual cortex," *Neuron*, vol. 45, no. 1, pp. 147–156, 2005.

[9] M. Siegel, M. R. Warden, and E. K. Miller, "Phase-dependent neuronal coding of objects in short-term memory," *Proc. Natl. Acad. Sci. U.S.A.*, vol. 106, no. 50, pp. 21 341–21 346, 2009.

[10] J. Pardey, S. Roberts, and L. Tarassenko, "A review of parametric modelling techniques for EEG analysis," *Med. Eng. Phys.*, vol. 18, no. 1, pp. 2–11, 1996.

[11] S. Y. Tseng, R. C. Chen, F. C. Chong, and T. S. Kuo, "Evaluation of parametric methods in EEG signal analysis," *Med. Eng. Phys.*, vol. 17, no. 1, pp. 71–78, 1995.

[12] W. Nho and P. J. Loughlin, "When is instantaneous frequency the average frequency at each time?" *IEEE Signal Process. Lett.*, vol. 6, no. 4, pp. 78–80, 1999.

[13] D. S. Rizzuto, J. R. Madsen, E. B. Bromfield, A. Schulze-Bonhage, D. Seelig, R. Aschenbrenner-Scheibe, and M. J. Kahana, "Reset of human neocortical oscillations during a working memory task," *Proc. Natl. Acad. Sci. U.S.A.*, vol. 100, no. 13, pp. 7931–7936, 2003.